EFFECTIVENESS OF METFORMIN ENGINEERED POLYMERIC NANOPARTICLES ON VIABILITY OF HEPATOCELLULAR CARCINOMA CELLS.

Tarek Aboushousha[1], Samah Mamdouh[2]*, Abdullah E. Gouda[2], Noha Said Helal[1], Hanem Hassan[2], Mohamed Abbas Shemis[2]

Article History: Received: 15.06.2023 **Revised:** 25.07.2023 **Accepted:** 01.08.2023

Abstract

Background: Hepatocellular carcinoma (HCC) is the most invasive form of liver cancer. Despite major improvements in diagnosis and treatment of early HCC, the prognosis is still very poor. The current targeted therapy generally has low tumor response rates and substantial side effects, so it is necessary to explore other types of targeted therapy against HCC. Metformin (Met) is a first-line anti-diabetic drug for the treatment of type 2 diabetes. It protects the liver from chemicals or viral hepatotoxicants. As a result of progress in nanotechnology; highly improved materials for biological purposes have been produced.

Aim: This study aims to model Met-loaded with natural chitosan polymer (Cs) and synthetic polymer (PCL) nanoparticles (NPs) and investigate the enhanced effect of polymers-Met blends on $HepG_2$ cells *in vitro*, and to examine the effect of Met on the $HepG_2$ growth, proliferation and apoptosis.

Methods: HCC ($HepG_2$) cell lines were treated with both free-Met and Met-conjugated withNPs (Met-Cs NPs and Met-PCL NPs), then the cell viability was measured. In addition, immunohistochemical (IHC) examination for cyclin D1, caspase-3, and ki67 was performed on HepG2 cell lines.

Results: The range of cell viability percentages for free-Met was 30.54-63.40 %, for Met-Cs NPs was 25.73-58.50%, and for Met-PCL NPs was 44.9-91.49%. Histopathological examination revealed degeneration and necrosis of HepG2 cells in Met-treated media (free-Met and nanoconjugated-Met NPs). By IHC; Met-treated media showed decreased expression of cyclin D1, as an indicator for cell growth limitation, decreased expression of k-i67, as an indicator for inhibited cell proliferation, and increased expression of caspase-3 which reflects increased apoptotic activity of Met.

Conclusion: The natural polymer chitosan (expressed by Met-Cs NPs) enhances the anticancer activity of the metformin drug and is completely safe on normal cells.

Keywords: HCC, *in vitro*, metformin, chitosan.

1.Department of Pathology, Theodor Bilharz Research Institute, Giza, Egypt
2.Department of Biochemistry and Molecular Biology, Theodor Bilharz Research Institute, Giza, Egypt

DOI: 10.31838/ecb/2023.12.9.182

Introduction

Hepatocellular carcinoma (HCC) represents 85%-90% of primary liver tumors. Globally, it represents the seventh most common cancer and the second most common cause of cancer-related deaths **(Ali et al, 2023).**

The global burden of HCC is increasing and the World Health Organization (WHO) approximates that above 1 million people will die from HCC in 2030 **(Zhang et al, 2022).** In Egypt, HCC is considered the most challenging health problem representing 23.8% of the total malignancies and ranks the fourth most common cancer **(Rashed et al, 2020).**

Many risk factors are associated with HCC; mainly hepatitis B virus (HBV) and hepatitis C virus (HCV) infection; where 50% of HCC cases are associated with HBV infection and 25% are associated with HCV **(Ezzat et al, 2021).** Other causes include autoimmune hepatitis, primary biliary cirrhosis, alcoholic cirrhosis, and non-alcoholic steatohepatitis **(Sharma and Nagalli, 2022).** In recent years, non-alcoholic fatty liver disease (NAFLD) and its more active form, non-alcoholic steatohepatitis (NASH) have emerged as new risk factors for HCC particularly in developed countries **(Foerster et al, 2022).** Additionally, diabetes mellitus and obesity have been correlated

with an increased risk of HCC **(Nakatsuka et al, 2023).**

Type 2 diabetes mellitus (T2DM) has a tremendous impact on human health worldwide **(Goyal 2023).** The global prevalence of T2DM in 2019 was estimated to be approximately 9.3%, and the incidence is expected to continue to increase **(Saeedi et al, 2019).**

Epidemiologic evidence suggests that patients with diabetes have an increased risk of many kinds of cancer including breast, pancreatic, lung, colorectal, kidney, and liver cancer **(Pati et al, 2023).** The link between diabetes and HCC was first reported approximately 40 years ago. In **1986 Lawson et al,** observed a 4-fold excess of diabetes incidence among patients with HCC.

The choice of HCC therapy is mainly challenged and based on many factors such as the stage of cancer, the severity of the underlying liver disease, the availability of treatment resources, and clinical expertise **(Lin et al, 2012).** HCC treatment can be classified into three categories: potentially curative, palliative, and symptomatic **(Izabela et al, 2021).** Potentially curative treatments including liver resection, transplantation, and local ablation are associated with promising 5-year survival rates of up to 75% **(Lin et al, 2012).** Unfortunately, the majority of HCC patients are subjected to palliative or symptomatic treatment **(Norman et al, 2022).** The 3-year survival rate for palliative treatment is 10–40%, and the duration of survival for patients who receive symptomatic treatment is <3 months **(Jordan et al, 2020).**

In tumors, the signaling pathways mediate proliferation and other processes involved in tumor progression and metastasis **(Sever et al, 2015).** The tumor growth induced by mitogenic compounds is associated with the activation of several cytosolic proteins, including those involved in the phosphorylation and activation of Mitogen-activated protein kinases (MAPKs) **(Cargnello et al, 2011).**

Metformin (Met) belongs to a biguanide class of oral hypoglycemic agents and is the first-line drug for the treatment of T2DM **(Ganesan et al, 2023)**. Moreover, metformin is a powerful anticancer agent that hinders cell proliferation via G1 phase arrest and also induces apoptosis, thus reducing the risk of HCC occurrence **(Cunha et al, 2020)** and **(Szymczak et al, 2023)**.

Several *in vitro* and *in vivo* studies have shown that metformin could exert its antitumor effect by targeting multiple pathways such as cell cycle/apoptosis, anti-inflammatory pathway, insulin/IGF-IR, and angiogenesis. Additionally, metformin helps lowering blood glucose levels throughout the day by reducing the liver blood glucose-raising effect. Rather than stimulating the release of insulin. Moreover, metformin increases the body sensitivity to insulin and therefore has benefits for weight management **(Vacante et al, 2019).**

However, owing to its low bioavailability and short half-life span, metformin monotherapy is imperfect, and its therapeutic efficacy is dependent on glucose levels at the tumor site **(Zhang et al, 2023).** Thus, a good carrier (drug delivery system) is needed for high loading and to diminish the limitations of Met's poor bioavailability and short half-life (**Javidfar et al, 2018; De et al, 2023**). Under high glucose conditions, metformin inhibits proliferation but does not induce cell apoptosis **(Samuel et al, 2019).** Consequently, reducing the glucose level at the tumor site is required for metformin to achieve anti-proliferation and apoptotic functions and provide effective cancer management.

Different studies tried novel methods to encapsulate metformin using various polymers and they revealed the outstanding effect of polymeric nanoparticles to overcome the metformin limitations **(Sartaj et al, 2021). Corti et al., 2008** developed sustained-release matrix tablets of metformin hydrochloride in combination with triacetyl-beta-cyclodextrin. The release studies of this report demonstrated that blends of hydrophobic swelling polymer (hydroxypropyl methylcellulose or chitosan) with a pH-dependent one (Eudragit L100-55) were more useful than single polymers in controlling drug release. Metformin was encapsulated in lecithin (LC) and chitosan (Cs) nanoparticles (NPs) to inhibit colorectal cancer (CRC) proliferation through modulations of long noncoding RNAs (lncRNAs), micro RNAs (miRNAs), and some biochemical markers. They concluded that the NPs can potentially be cytotoxic to CRC cells *in vitro* by modulating noncoding RNA (**Abd-Rabou et al, 2021**).

Chitosan and its derivatives are gaining admiration and are widely used as a carrier for various novel dosage forms generally due to their cationic nature and endosomal escape, biodegradability, low cost, and therapeutic efficacy. The chitosan characteristics improve the solubility

of poorly soluble drugs, in addition to controlling the release of drugs by slow erosion from hydrated matrix (**Wang et al, 2015**). While, chitosan and hydroxy propyl methyl cellulose phthalate (HPMCP), an enteric coating polymer were used as matrix materials for metformin delivery and extended-release was obtained. Another WZB117 decorated metformin-carboxymethyl chitosan nanoparticles for targeting breast cancer metabolism were fabricated with extended-release for up to 60 hours, indicating growth-inhibitory and apoptotic characteristics (**Garg and Saluja, 2013; De et al, 2023**).

This study aims to fabricate metformin polymeric nanoparticles and observe the aspects of the drug delivery system related to the type of polymer. The aim extends to investigate the enhanced effect of polymers-Met blends on $HepG_2$ cells *in vitro*, and examine the effect of Met on the $HepG_2$ growth, proliferation and apoptosis. This will further point out the most promising strategies in the experiments, to overcome the limitations of metformin's poor bioavailability and short life-span.

MATERIALS AND METHODS:

Materials:

Poly -ε-caprolactone (PCL), polyvinyl alcohol (PVA), dichloromethane (DCM), stearic acid, polyethylene glycol (PEG), chitosan, low molecular weight, deacetylated chitin, poly (D-glucosamine), glacial acetic acid and sodium tripolyphosphate (TPP) were purchased from Sigma-aldrich (Germany). Phosphate buffer saline (PBS), sodium hydroxide, and hydrochloric acid were supplied by Loba Chemical (India). Metformin (Met) was purchased fromEl-Nasr Pharmaceutical Chemical Co. (Egypt). Ultrapure water with resistivity of 18 MU cm was used in all aqueous preparations.

Methods:

Preparation of Met-polymer nanoparticles

Together with using both natural chitosan polymer(Cs) and synthetic polymer (PCL), two novel techniques were conducted to fabricate metformin-polymer NPs.

Met-PCL NPs were prepared by a polymer-to-drug ratio of 1:1. A weight of 100 mg of Met was dissolved in the aqueous phase (2 ml PVA). Likewise, 100 mg PCL was liquefied in 8 ml dichloromethane (DCM). The aqueous phase was added to the organic phase (DCM) and homogenized using a high-speed homogenizer for 3 min at 5000 rpm in the presence of 2 ml stearic acid that stabilize the boundary of the internal water in oil emulsion (w1-o). The resulting emulsion was transferred into a larger flask containing an aqueous solution of {25 ml (2 % PVA), 10 ml (0.3 % Cs), and 5 ml (0.5 % PEG)} and a drop of Tween 80 was added to stabilize the boundary of the oil in water emulsions (o-w2). The mixture was homogenized for 5 minutes at 8000 rpm to form the second emulsion water-in-oil-in-water (w1-o-w2). All the previous steps were repeated without the addition of the drug for the preparation of empty PCL nanocapsules. The whole process of homogenization was done on ice and all experiments were performed in triplicate. The prepared nanoemulsion was kept on a magnetic stirrer overnight at 1000 rpm at room temperature to evaporate the DCM. Then centrifuged using a high-speed cooling centrifuge at 10°C and 13000 rpm for 45 min (**Tshweu et al, 2013**).

The Met-Cs NPs were prepared according to a slightly modified ionotropic gelation method using the natural polymer Cs and TPP as a cross-linker. Particles with and without Met were prepared in the same conditions. The unloaded Cs particles were used as a negative control. Briefly, 2 mg/ml Cs in 1% (v/v) acetic acid and 1mg/ml of TPP aqueous solution were prepared and filtrated using a 0.22 μm syringe filter (Millipore, USA). The pH level of both Cs and TPP solutions were adjusted to 5.5 by the addition of NaOH and HCl, respectively. For the experiments with encapsulated Met, the Met was dissolved into the Cs solution to a concentration of 2 mg⁄ml (Cs to Met weight ratio of 1:1). A glass burette was adjusted to add the TPP solution to the Cs-Met solution (at Cs to TPP weight ratio of 2:1) drop wisely with the flow rate of 1.25 ml/min. During the addition, the Cs solution was stirred vigorously (1000 rpm) using a magnetic stirrer. The solution was mixed for an additional 10 min after all of the TPP was consumed. The nanoparticle blend was incubated at 4°C for 40 min, and then centrifuged at 18,000 rpm for 30 min at 4°C. The supernatant was collected for calculating the efficiency of entrapment and the nanoparticles pellet was washed three times with double distilled water to remove the unreacted metformin. All experiments were done at room temperature (**Calvo et al, 1997; Neves et al, 2014**).

Subsequently, the nanoparticles pellet was resuspended in double distilled water (50 mg/ml) and stored at -80°C till freeze-dried. The resuspended pellet was frozen overnight at -10°C. Subsequently, the samples were transferred to the freeze dryer under the standard freeze-drying

conditions (pressure 7 bars, the inlet temperature was 96ºC, and the achieved outlet temperature ranges from 65-70°C).

Determination of encapsulation efficiency and drug loading percentages

Exactly 2 mg of the Met-PCL NPs and Met-Cs NPs were dissolved in 1 ml deionized water. Then incubated at 37°C for 20 min and centrifuged at 10,000 rpm for 10 min. The absorbance of the supernatant was measured at 232 nm. The samples were measured in triplicate and the results were quantified as the mean ±SD. These Met quantities were determined according to a calibration curve, which was plotted by measuring the UV absorbance of known Met concentrations (15.625, 7.813, 3.906, 1.953, 0.997) µg/ml (Fig. 1a). These standards were prepared using 1x PBS buffer of pH 7.4 and absorbance was determined using a Multiskan sky spectrophotometer (Thermo Scientific, Germany).

The EE was calculated using the following equation:

Encapsulation efficiency (EE %) = (Wi-Wt)/Wi ×100% (Eq1).

Where wi is the initial weight of the Met added during the preparation step and wt is the weight of the drug in the nanocapsule.

The drug loading percent was calculated using the following equation:

The drug loading % =(The weight of the Met in NPs)/(The total weight of the NPs) x 100 (Eq 2).

Determination of the particle size, particles size distribution, and zeta potential

Malvern Zetasizer Nano ZS (Malvern instruments ltd., Malvern, Worcestershire, UK) was used to measure the particle size distribution, zeta potential, and polydispersity index (PDI). Typically, 2 mg of PCL, Cs, Met-PCL, and Met- Cs NPs were resuspended in 2 ml of 1% acetic acid solution; it was sonicated for 10 min to confirm uniform dispersion. The particle size analysis of the NPs was accomplished in triplicate at 25°C, an angle of 90° for the photomultiplier, and a wavelength of 633 nm. The surface charge (zeta potential) of the nanoparticles was quantified from the electrophoretic mobility. The zeta potential measurements were performed at pH 5.5 in triplicate using the 100 μL aqueous dip cell by Zetasizer, Nano ZS (Malvern Instruments Ltd., Malvern, Worcestershire, UK). The samples were diluted 1:100 with double distilled water before measurements.

***In vitro* drug release of Met-Cs**

Initially, 5 mg of Met- Cs NPs and Met-PCL NPs, were added to 5 ml 1x PBS buffer of pH 7.4 and pH 5.5. The mixture of the resuspend particles was incubated at 37°C in an orbital stirring shaker at 100 rpm. Aliquots of supernatant (500 µl) were taken out at time intervals and the particle mixture was supplemented with 500 µl fresh 1x PBS buffer (pH 7.4 and 5.5) to maintain the total initial volume. The absorbance of released Met at pH 7.4 and pH 5.5 was measured using Multiskan sky spectrophotometer (Thermo Scientific, Germany), at λmax = 232 nm with the same calibration curve used to calculate the entrapment efficiency **(Fig. 1a)** together with another one plotted at pH 5.5 **(Fig. 1b).**

Concentration (µg/ml)	Optical density
0.997	0.06
1.953	0.14
3.906	0.26
7.813	0.49
15.625	0.92

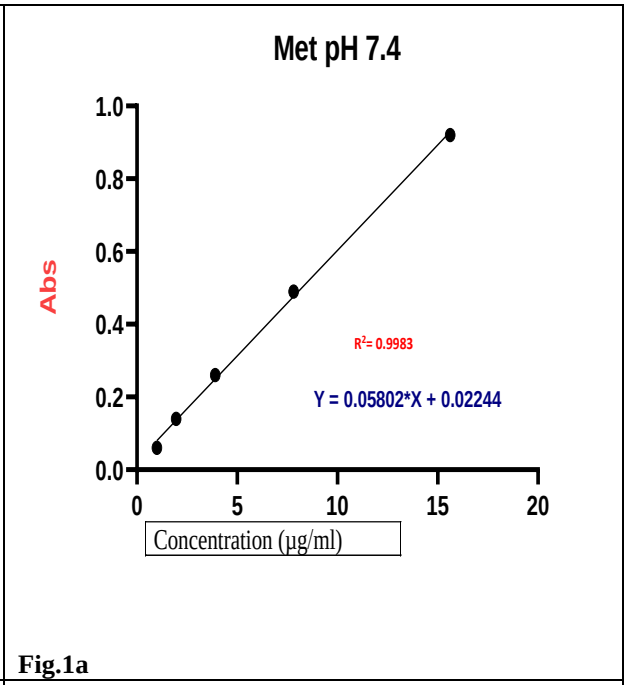

Fig.1a

Concentration (µg/ml)	Optical density
0.997	0.55
1.953	0.134
3.906	0.246
7.813	0.51
15.625	0.94

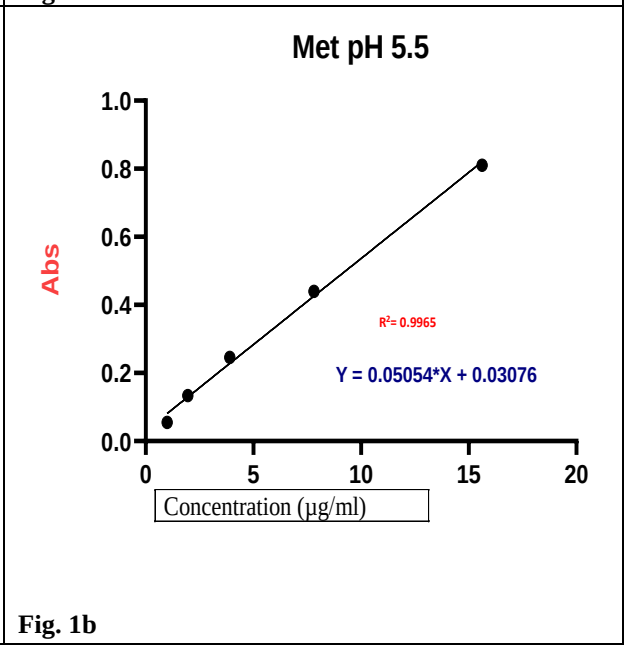

Fig. 1b

Fig. 1: Metformin calibration curve (**a**): Metformin calibration curve at pH 7.4, (**b**): Metformin calibration curve at pH 5.5.

***In vitro* cytotoxicity studies of Met-polymeric NPs using Vero and HepG2 cell lines**

Human liver cancer cells (HepG2) and normal cells (Vero) were obtained from VASCERA Co. (Vaccine sera and Drugs, Giza, Egypt) and supplied from the American Type Culture Collection (Manassas, VA, USA). Cells were cultured using DMEM and MEM. All media were supplemented with 10% fetal bovine serum (FBS), and 1% penicillin/streptomycin. Cells were incubated at 5% CO_2 and humidified at 37°C for growth maintenance. A 100 ml sample of cells at a density of 10^4 cells was plated in a 96-well culture plate and then incubated for 24 hours at 37°C to attain 85% confluency. Serial dilutions of each drug (free Met, Met-Cs, free Cs, Met-PCL, and free PCLNPS) were prepared using maintenance growth media (MEM for Vero and DMEM for HepG2) to produce standard solutions that are further used for the cytotoxicity assay as follows: (2, 1, 0.5, 0.25, 0.125, 0.062, and 0.031 mg/ml). Aliquots of 100 µl sample of each substance concentration were added to each well containing cells. A well of only media as negative control and another one as blank, were prepared in triplicate, then incubated for 48 hours at 37°C and the medium was replaced with 200 ml of

fresh medium. Cytotoxicity was performed using Vybrant MTT assay following the manufacturer's protocol. The absorbance was measured at 490 nm using a microplate reader (Molecular Devices Co., CA, United States) and a reference wavelength of 655 nm. The cell viability percentage was calculated compared to control.

Cell culture

The HepG2 cells were grown in DMEM low glucose media containing 10% FBS and 1% penicillin/streptomycin, and incubated at 5% CO_2 humidified at 37°C. Then, 500 µl of cells were plated in 24 well culture to get a cell count of 500,000/well. The cells were incubated for 24 hours at 37ºC to reach 85 % confluency. The doses (IC_{50}) of Met and Met-Cs NPs were added to the plate. The plates were incubated for 24 hours at 37ºC. After incubation of the cells with the test substance, the medium was aspirated from the wells. Cells were collected for histopathological studies.

Histopathological technique

Histopathological examination of tissue is a direct method for analyzing the morphology of cells. HepG2 cells were collected from the culture and processed in the same way as tissue specimens by embedding them in agarose and subsequently in paraffin as cell blocks. This approach has the benefit of allowing several sections to be cut from a single cell block **(Koh, 2013).**

Preparation of formalin-fixed paraffin blocks from HepG2 cells

This technique results in cell culture preparation that mimics the histologic processing of tissue samples, allowing the cell culture to be used as a control for tissue immunohistochemistry (IHC). Two 150 cm^2 flasks of near-confluent cell culture were used, the volume of the packed cell pellet ideally was approximately 0.5 ml, media was aspirated off cell pellet. Then, 20 ml of neutral buffered formalin were added slowly down the side of the tube to avoid disturbing the pellet, the cells were fixed in formalin overnight at 4ºC.

Delivery of the preparation could be made within 24 hours of the start of fixation, but if not, the formalin could be removed and replaced with 20 ml of 70% ethyl alcohol (EtOH) without resuspending the pellet. This acted as a non-cross linking preservative, and the cells can be kept this way indefinitely at 4ºC without freezing. Then the formalin was removed and replaced with 20 ml of 70% EtOH without the pellet being resuspended. The cells were preserved at 4ºC. The cell pellet was then processed into a paraffin block that was cut into 3-5 micrometer thick slices on positively charged glass slides and stained with hematoxylin and eosin for histopathological examination.

The tissue sections were examined by using light microscope (Scope A1, Axio, Zeiss, Germany). Photomicrographs were taken using a microscope camera (AxioCam, MRc5, Zeiss, Germany).

Immunohistochemical analysis

Immunohistochemical study was done for the examination of cyclin D1 as a promotor of the cell cycle, caspase-3 as a marker for apoptosis, and Ki67 as a proliferation marker.

Sections prepared from the cell blocks of different groups were processed for IHC analysis, first unmasking for antigens was performed with 10 mM sodium citrate buffer, pH 6.0, at 90°C for 30 min. Sections were incubated in 0.03% hydrogen peroxide for 10 min at room temperature to remove endogenous peroxidase activity, and then in blocking serum (0.04% BSA, A2153, Sigma-Aldrich, Shanghai, China, and 0.5% normal goat serum X0907, Dako Corporation, Carpinteria, CA, USA, in PBS) for 30 min at room temperature. The sections were incubated overnight at 4°C with cyclin D1 antibody (Code Number# M3642, rabbit IgG, concentrated, anti-human, DAKO), at a dilution of 1:100, caspase-3 antibody (#31A1067): sc-56053, concentrated, Sant Cruz.) at a dilution of 1:100, and Ki-67 antibody (Roche, anti-Ki-67, Rabbit Monoclonal Primary Antibody, Cat. Number: 790-4286) at a dilution of 1:200. After 24 hours, sections were washed three times for 5 min in PBS. Non-specific staining was blocked by 5% normal serum for 30 min at room temperature and sections were then incubated for 20 min at room temperature with the secondary antibody (link) provided by Envision Kit (Dako-Denmark). Finally, staining was developed with diaminobenzidine substrate and sections were counterstained with hematoxylin. Negative controls were carried out in which PBS was used instead of the primary antibody **(Aboushousha et al, 2018).**

Immunohistochemical interpretation

The cyclin D1 and caspase-3 positive staining was indicated by brown cytoplasmic, membranous, or both staining of tumor cells. The score used according to **Morinaga et al, (2008)** is the number of positive cells evaluated under x400 magnification (extent of expression) and was assessed as: 0 = no positive cells; 1+ = 1-10% positive cells; 2+ = 11-50% positive cells, 3+ = > 51% of cells with positive staining.

The ki-67 index was obtained by the percentage of tumor cells that were labeled at nuclei by Ki-67 **(Shi et al, 2015).**

Statistical analysis

The data were presented as the mean ± SD. The test of significance was performed by GraphPad Prism 8 (San Diego, California, USA) using XY analysis (Fit spline/LOWESS and correlation). The p*< 0.05 was considered a statistically significant difference.

Results and discussion:

Encapsulation efficiency and drug loading percentages

The entrapment efficiency (EE) of the Met-Cs NPs was measured as 91.42± 4.22% and the loading capacity was 89.82± 3.92%. This percentage reveals the nano-chitosan as a perfect carrier for the delivery of metformin. Because the ionic gelation principle depends on the ionic interaction of the positively charged amine groups of chitosan and metformin with negatively charged TTP cross linker, the chitosan percentage affects the entrapment efficiency of the recovered particles. A viscous solution (2 mg/ml) of chitosan that might causes effectively dispersion of metformin into the polymer matrix increasing both the efficiency of entrapment and loading capacity. These results agree with the previously published by **Elkomy et al, 2021** who stated that both the entrapment efficiency and the loading capacity were raised to 91% when the chitosan: metformin: TPP ratio was 1:1: 0.5. This study also, outperformed another report by **Kalpna et al, 2018** who reported 83.17% entrapment efficiency and 82.17±2.21 drug loading at the same ratios of chitosan: metformin: TPP and increasing the TPP ratio to 1 gave rise to EE of 94.05 % and LC of 70.26±0.3. An earlier study examined different polymers to encapsulate metformin and the chitosan polymer showed the highest drug loading compared to Ethyl cellulose (EC), poly (lactic-co-glycolic acid) (PLGA), poly (methyl methacrylate) (PMMA) (**Duarah et al, 2015**). All the above studies reveal the outstanding characteristics that support chitosan to be a good carrier for metformin. For the PCL-metformin NPs, the encapsulation efficiency and the loaded capacity were found to be 99.1% and 49.5% respectively. Thes results indicate that the double emulsion method is a powerful technique for encapsulation both hydrophilic and hydrophobic drugs.

Characterization of the metformin-polymer nanoparticles

In this study, we used the double emulsification (w1-o-w2) and the ionic gelation techniques to fabricate polymeric nanocarriers for improving the metformin efficacy. The mean particle sizes of the polymeric nanocapsules should be within the range of 250-500 nm but, in some cases, it is possible to obtain low mean particle sizes by using ultrasound in the initial steps of the procedures (**Mora-huertas et al, 2010**). The dynamic light scattering illustrated the homogenous particle size distribution of free polymers and Met-polymers NPs, where the DLS particle size patterns showed one peak at 101.7 nm and 97.23 nm for the free PCL and Met-PCL NPs with zeta potential of 27.5 mV and 24.6 mV respectively **(Fig. 2a, 2b, 2c and 2d).**

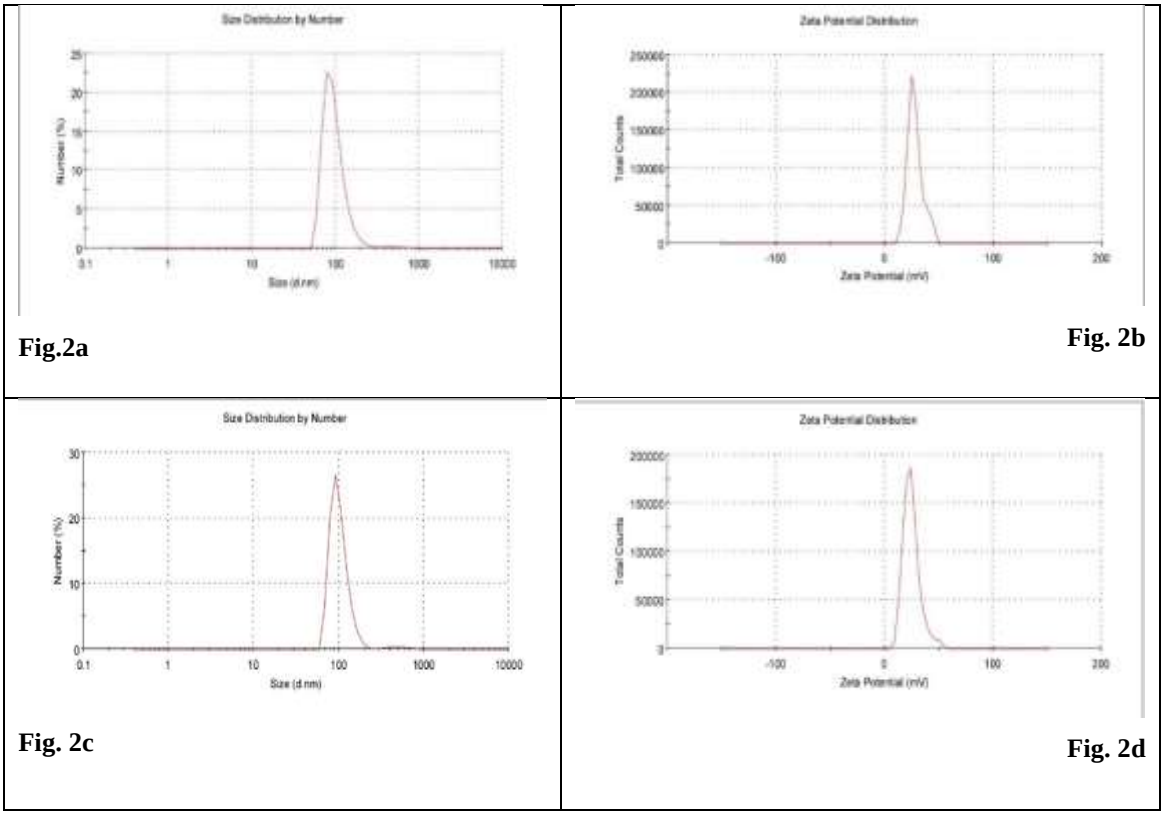

Fig. 2: (**a**): Particle size of free PCL**,** (**b**): Zeta potential of free PCL**,** (**c**); Particle size of Met-PCL and (**d**): Zeta potential of Met-PCL**.**

Also, small particle sizes were obtained for Cs and Met-Cs NPs. The pattern showed one peak at 108 nm and 114 nm for free Cs and Met-Cs with zeta potential of 26.2 mV and 24.9 mV correspondingly (Fig. 3a, 3b, 3c and 3d). The small particle sizes obtained in this study may be due increasing the stirring speed of Cs-Met mixture before and during the addition of TPP solution. Also, controlling the homogenization speed in the double emulsion method can affect the particle size. That is why, the results of the current study outperformed the previous one reported by Tshweu et al, 2020 who stated that the PCL (PEG–Mox) NPs were 241.8 ± 4 nm in diameter, significantly larger than the 174.4 ± 10 nm of empty PCL NPs. The high zeta potential value of both free PCL, free Cs, Met-PCLand Met-Cs NPs revealed a huge surface area of the NPs that prevents particle agglomeration and shows the very high chemical activity and its stability in solution. The positive charge was due to the adsorption of chitosan on the surface of the nanocapsules. The homogenous particle size distribution of free polymers and Met-polymers NPs indicates that the metformin fine powder loading did not affect the particle size distribution or slightly increased the particle size by means of 4 to 6 nm. These results are agreed with the previous reported by Yadav et al, 2021 who noticed that the blank chitosan NPs showed slightly less particle size and zeta potential as compared to BSA-loaded NPs. Whereas Piras et al, 2015 stated that the particle size was shifted from 124 to 185 nm when loaded with the antimicrobial peptide temporin B.

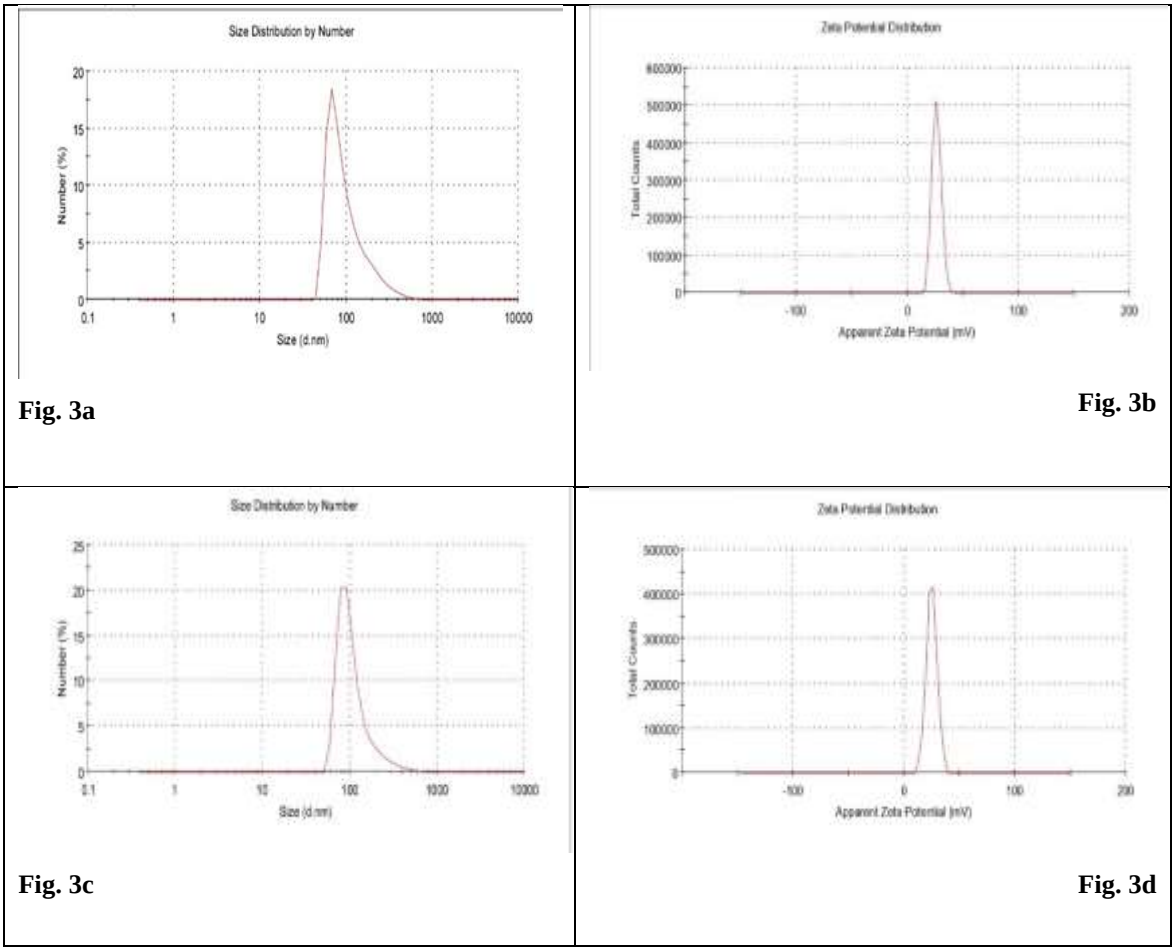

Fig. 3a **Fig. 3b**

Fig. 3c **Fig. 3d**

Fig. 3: (**a**): Particle size of free Cs, (**b**): Zeta potential of free Cs, (**c**): Particle size of Met-Cs and (**d**): Zeta potential of Met-Cs.

In vitro drug release of the Met-polymers nanoparticles

The release of drugs from the chitosan nanoparticle is affected by the hydrophilicity of chitosan and the pH of the swelling solution. Hence, an improved drug release could be achieved when polymers get into contact with an aqueous medium, the water would diffuse into the polymer until the polymer swells, chitosan release mechanism involves swelling, diffusion of drugs through the polymeric matrix and polymer desolation (**Younis et al, 2018**). Due to the hydrophilicity of chitosan, Cs-NPs exhibit pH-dependent drug and controlled drug release system (**Mohammed et al, 2017**). In this study, the *in vitro* release profile of Met-Cs NPs in PBS at pH 7.4 and pH 5.5 was studied over a period of 24 hours. At pH 5.5, the Met-Cs NPs showed an initial release of 10.5± 0.55% within the first 6 hours, 26.73% ± 1.54% after 12 hours, 71.54% ± 5.3% and a cumulative release of 97.6 ± 2.67% in 24 hours and lower concentrations were released from the met-Cs NPs at pH 7.4 within 6, 12 and 18 hours but the total metformin loaded was completely released within 24 hours at the two different pH **(Fig. 4 a).** The exponential pattern demonstrated by the release profile of Met-Cs NPs indicates that the system is suitable for sustained release of therapeutics. The amount of metformin and chitosan as well as the degree of deacetylation of chitosan play a vital role in the release rate. The higher deacetylation of chitosan, the higher the number of amino groups that forms ionic interactions with the negatively charged TPP, resulting in the formation of condensed particles, this results in lowering the permeability of nanoparticle surface and decrease in release rate. The larger the amount of metformin-encapsulated leads to higher diffusion rate due to the formation of concentration gradient between the chitosan and buffer matrix (**Kafshgari et al, 2012**). The results of Met-Cs *in vitro* drug release are in accordance to the previously published results by **Duarah et al, 2015,** who studied different polymers to encapsulate metformin and the chitosan polymer, they showed the highest drug loading compared to EC, poly (lactic-co-glycolic acid) (PLGA), poly (methyl methacrylate) (PMMA). The results

clarified the highly mannered controlled release within 22 hours for all polymers. Also, our results outperformed the previously published studies that showed complete metformin release from the chitosan microspheres within 12 hours (**Kalpna et al, 2018**).

The Met-PCL NPs showed a very delayed *in vitro* metformin release at the two different pH within the first 8 hours followed by controlled release till 18 hours, then the whole metformin amount was released by 24 hours **(Fig. 4b).** These results go parallel with those formerly issued by **Abdelghany et al, 2021,** who investigated 80% of the amoxicillin release from the PCL polymer NPs actually within 14 hours.

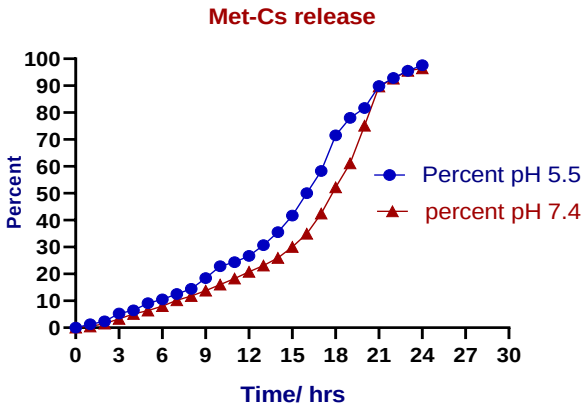

Fig. 4a

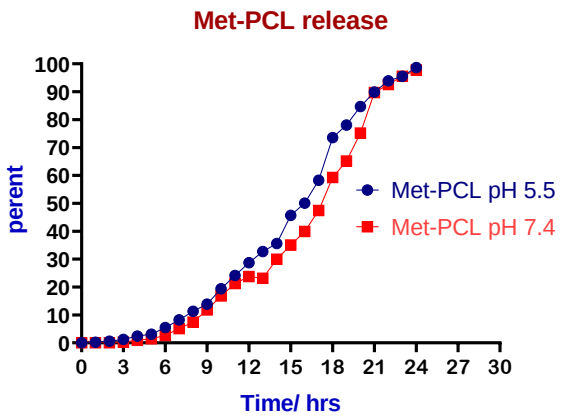

Fig. 4b

Fig. 4: (**a**): *In vitro* drug release of Met-Cs NPs and (**b**): drug release of Met-PCL NPs.

In vitro cytotoxicity studies of Met-polymeric NPs using the Vero and HepG2 cell lines

In the present study, Vero cell line was treated with free Met, Met-Cs, free Cs, Met-PCL and free PCL NPs with a concentration ranging from 2 to 0.03125 mg/ml and showed cell viability ranging 55.54–88.40 % for free Met, 54.73– 92.50% for Met-CS NPs, 69.9–94.49% for Met-PCL NPs, 81.24–99.25% for free Cs and 81.55–98.41% for free PCL as shown in **Table 1, Fig. 5.** Also**,** HepG2 cell line was treated with the same concentration of each parameter and displayed cell viability ranging 30.54–63.40 % for free Met, 25.73–58.50% for Met-Cs NPs, 44.9–91.49% for Met-PCL NPs, 51.24–81.25% for free Cs and 81.55–99.41% for free PCL as shown in **Table 2, Fig. 6.**

Data obtained from statistical analysis using graph pad prism statistics version 8 showed P-values of < 0.05, which means that there were significant differences between the viability percentage of free Met, Met-Cs, free Cs, Met-PCL, and free PCL NPs on the Vero and HepG2 cell lines.

Table 1:Viability % of free Met, Met-Cs, free Cs, Met-PCL and free PCL NPs on Vero cell line.

Concentration (mg/ml)	Viability % of Vero cell line				
	Met	Met-Cs	Met-PCL	Cs	PCL
2	55.54	54.73	69.9	81.24	81.55
1	59.58	56.65	72.1	89.45	86.22
0.5	65.97	69.19	77.4	90.77	88.125
0.25	74.57	78.26	84.79	95.44	92.09
0.125	82.44	81.67	87.84	94.99	95.88
0.0625	86.1	89.21	90.58	97.88	96.99
0.03125	88.4	92.5	94.49	99.25	98.41
Mean of viability	73.229±4.9	74.601±3.6	82.423±7.4	92.146±6.8	91.324±7.9

IC_{50} (mg/ml)	-----	-----	-----	-----	----
The correlation between the concentration and viability %	r=-1.372 P= 0.0085	r=-0.6149 P= 0098	r=-1.629 P=0.0061	r=0.2079 P=0.0033	r=-0.4107 P=.0029

Viability is represented as %, while the correlation coefficient (r)

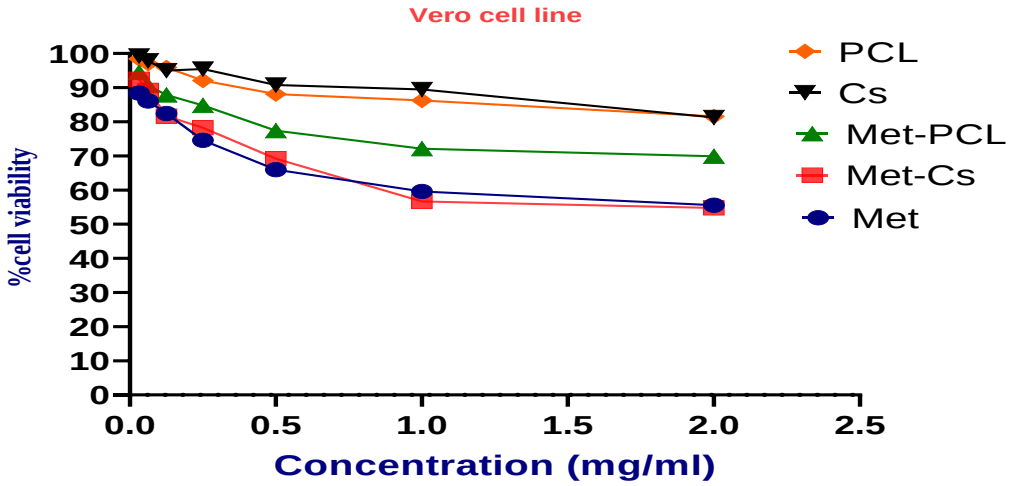

Fig. 5: Cell viability % of free Met, Met-Cs, free Cs, Met-PCL and free PCL NPs on Vero cell line.

Table 2: Viability % of free Met, Met-Cs, free Cs, Met-PCL and free PCL NPs on HepG2 cell line.

Concentration (mg/ml)	Viability % of HepG2 cell line				
	Met	Met-Cs	Met-PCL	Cs	PCL
2	30.54	25.73	44.9	51.24	81.55
1	34.58	31.65	47.1	59.45	87.22
0.5	40.97	39.19	52.4	61.77	88.125
0.25	49.57	47.26	84.79	65.44	92.09
0.125	57.44	49.67	85.84	71.22	95.88
0.0625	61.1	58.21	90.58	77.88	97.055
0.03125	63.4	58.5	91.49	81.25	99.41
Mean of viability	48.229±5.3	44.315±4.6	71.014±9.4	66.89±8.8	91.62±9.9
IC_{50} (mg/ml)	0.241	0.169	0.745	-----	----
The correlation between the concentration and viability %	r= -0.8835 P= 0.0084	r= -0.9115 P= 0.0043	r= -0.8409 P= 0.0178	r=-0.8772 P= 0.0095	r=-0.9179 P= 0.0036

Viability is represented as %, while the correlation coefficient (r).

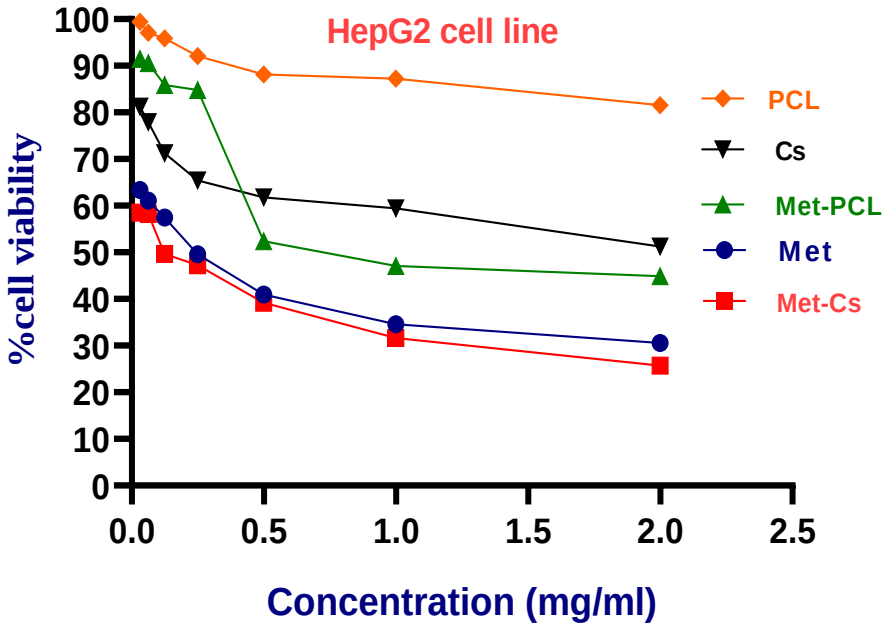

Fig. 6: Cell viability percent of free Met, Met-Cs, free Cs, Met-PCL and free PCL NPs on $HepG_2$ cells.

Histopathological and Immunohistochemical Results and Discussion

Histopathological examination of sections from different groups revealed that cells from the free metformin-treated culture media showed marked cellular degeneration and necrosis with distorted malignant acinar pattern **(Table 3, Fig. 7).**

This finding indicates the role of metformin in inducing a cytotoxic effect on HepG2 as reported by **Kim et al, 2021** and **Tawfik et al., 2022** who reported that metformin inhibits HepG2 cell viability. Moreover, other studies stated that metformin treatment has been associated with decreasing the occurrence of HCC **(Donadon et al, 2010 and Nkontchou et al, 2011).** This is attributed to its glucose-lowering effect which is caused by inhibition of hepatocyte gluconeogenesis **(Zhang et al, 2021).**

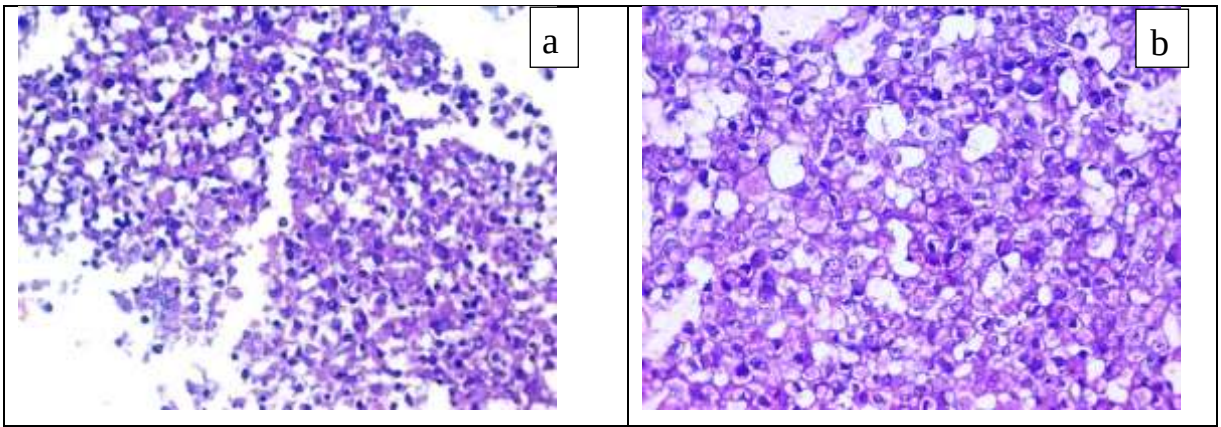

Fig. 7: Sections from cultured HepG2 cells. (a): free metformin: marked cellular degeneration and necrosis (b): Met-Cs: less degeneration and better preservation of HepG2 cells (H&E stain, X400)

Table 3: Histopathological features of untreated HepG2 cells, free Met and Met-Cs

	Free HepG2	Free-Met	Met-Cs
HepG2 cellularity	+++	+	++
HepG2 differentiation	+++	+	++
HepG2 degeneration	-	++	+

Immunohistochemical examination

The IHC results revealed that the expression of the cell cycle regulatory protein cyclin D1 was lower in Met-treated media groups (free-Met and Met-Cs) than in untreated HepG2. In addition, cyclin D1 was lower in free-Met than in Met-Cs. Our results are in agreement with the findings of **Sabry et al., 2019** who stated cyclin D1 expression was decreased in metformin HepG2 treated cells compared with the control. Also, **DePeralta et al., 2014** stated that metformin may inhibit HCC cell growth by downregulating cyclin D1.

Furthermore, **Vacante et al., 2019 and Cai et al., 2013** reported that treatment with metformin decreased HepG2 cell proliferation and restricted the cell cycle progression to the G0/G1 phase in hepatocellular cancer cells.

The expression of the pro-apoptotic protein caspase-3 was lower in Met-treated media groups (free-Met media and Met-Cs) than in HepG2 control media and was lower in Met-Cs than in free-Met. Contrary to our findings, **Sabry et al., 2019** stated that caspase-3 levels were increased in metformin treated HepG2 cells compared to control. This can be explained as metformin can induce apoptosis in a dose-dependent manner. **Zou et al., 2019** reported that the apoptosis rate in cancer cell lines increased with increasing concentration of metformin. A recent study by **Eskandari and Eaves, 2022** suggested a pro-survival role for caspase-3.

The expression of the proliferative marker ki-67 was lower in Met-treated media groups of HepG2 cells (free-Met and Met-Cs) than in HepG2 with control media. Furthermore, k-i67 was lower in free-MET than in Met-Cs. This indicates that when HepG2 cells treated with free or Met-Cs, the proportion of proliferating cancer cells decreases. Moreover, free metformin can induce more suppression of the proliferative activity of HepG2 compared to that induced by chitosan nanoconjugated metformin.

Our findings were in the same line with **Kim et al., 2021 and Sabry et al., 2019** who stated that metformin has an anti-proliferative activity in HepG2 cells and can inhibit liver cancer cell growth **(Table 4, Fig. 8).**

Table 4: Expression of Cyclin D1, Caspase-3 and Ki-67 in untreated HepG2 cells, free-Met and Met-Cs

Marker	HepG2 control	free metformin (Met)	Met-Cs NPs
Cyclin D1	90%	50%	70%
Caspase-3	10%	30%	50%
Ki-67	90%	60%	50%

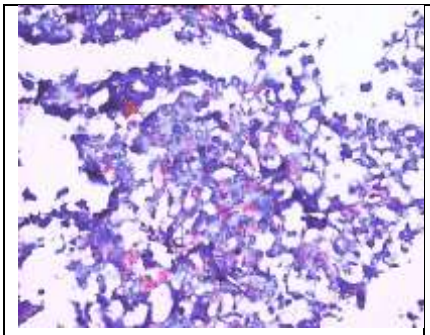

Cyclin D1 expression in untreated HepG2 cells

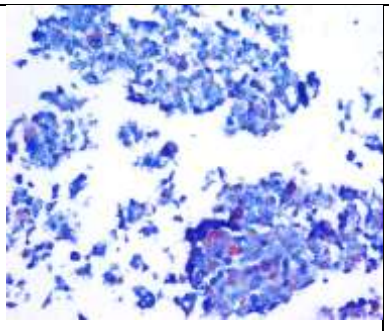

Cyclin D1 expression in free-Met

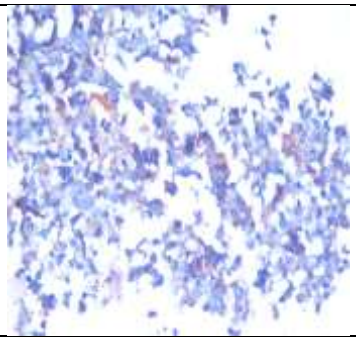

Cyclin D1 expression in Met-Cs

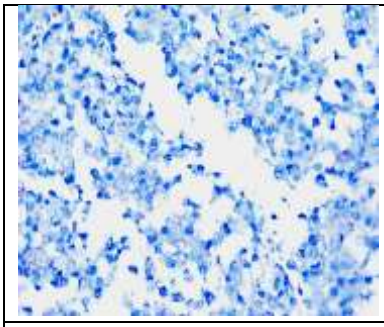

Caspase-3 expression in untreated HepG2 cells (10%)

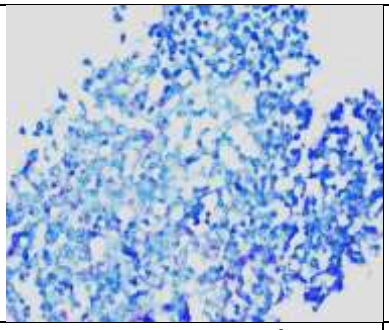

Caspase-3 expression in free-Met (30%)

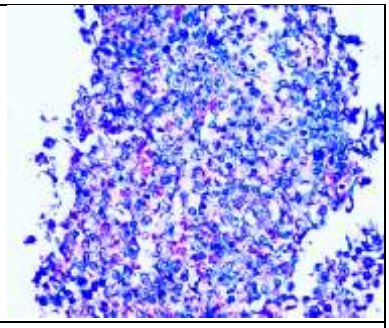

Caspase-3 expression Met-Cs (50%)

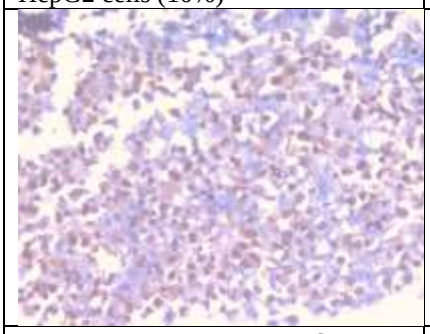

Ki67 expression in untreated HepG2 cells (90%)

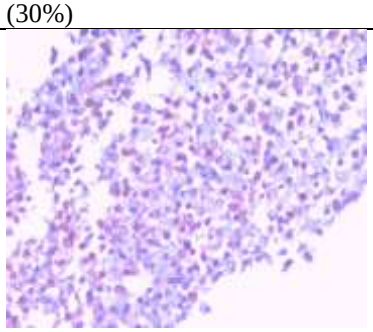

Ki67 expression in free-Met (60%)

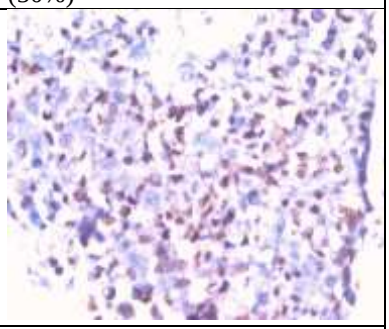

Ki67 expression in Met-Cs (50%)

Fig. 8: Expression of Cyclin D1, Caspase-3 and Ki-67 in untreated HepG2 cells, free-Met and Met-Cs.

In a conclusion, our data revealed that treatment of HepG2 cells with both free metformin and chitosan nanoconjugated metformin induces degeneration and necrosis of HepG2 cancer cells, an effect similar to chemotherapeutic drugs. Mechanistically, metformin treatments showed increased expression of caspase-3, as an indicator for induced apoptosis, and decreased expression of cyclin D1, as an indicator for cell growth limitation, as well as decreased expression of k-i67, as an indicator for inhibited cell proliferation. These findings may provide novel therapeutic targets or treatment strategies against HCC.

REFERENCES

- Abdelghany, A., El-Desouky, M. A., & Shemis, M. (2021). Synthesis and characterization of amoxicillin-loaded polymeric nanocapsules as a drug delivery system targeting Helicobacter pylori.Arab Journal of Gastroenterology, 22 (4). 278-284. ISSN 1687-1979 https://doi.org/10.1016/j.ajg.2021.06.002.
- Abd-Rabou, A. A., Abdelaziz, A. M., Shaker, O. G., &Ayeldeen, G. (2021). Metformin-loaded lecithin nanoparticles induce colorectal cancer cytotoxicity via epigenetic modulation of noncoding RNAs. Molecular biology reports, 48(10), 6805–6820. https://doi.org/10.1007/s11033-021-06680-8.
- Aboushousha T, Hammam O, Safwat G, Eesa A, Ahmed S, Esmat ME, Helmy AH. Differential Expression of RAGE, EGFR and Ki-67 in Primary Tumors and Lymph Node Deposits of Breast Carcinoma. Asian Pac J Cancer Prev. 2018 Aug 24;19(8):2269-2277. doi: 10.22034/APJCP.2018.19.8.2269. PMID: 30139236; PMCID: PMC6171384.
- Ali, A.A.K., Gamal, S.E., Anwar, R. *et al.* Assessment of clinico-epidemiological profile of Hepatocellular carcinoma in the last two decades. Egypt J Intern Med **35**, 18 (2023). https://doi.org/10.1186/s43162-023-00201-8.
- Elkomy, A., El-Zawahri, M. M., Amer, A.M. M., Aboubakr, M., Abdel Hakeem, M., Ismail, S. H., Mohamed, G. G., salem, A. M. (2021). Preparation and characterization of metformin-loaded chitosan nanoparticles for biomedical applications. Benha Veterinary Medical Journal 42 (1). 33-38.
- Cai X, Hu X, Cai B, Wang Q, Li Y, Tan X, Hu H, Chen X, Huang J, Cheng J, Cheng J, et al: Metformin suppresses hepatocellular carcinoma cell growth through induction of cell cycle G1/G0 phase arrest and p21CIP and p27KIP expression and downregulation of

cyclin D1 in vitro and in vivo. Oncol Rep 30: 2013; 2449-2457. doi.org/10.3892/or.2013.2718

- Calvo, P., Remuñan-Lopez, C., Vila-Jato, J L., & Alonso, M J. (1997). Novel hydrophilic chitosan poly ethylene oxide nanoparticles as protein carriers. Journal of Applied Polymer Science. 63: 125-132.
- Cargnello M, Roux PP. Activation and function of the MAPKs and their substrates, the MAPK-activated protein kinases. Microbiol Mol Biol Rev. 2011 Mar;75(1):50-83. doi: 10.1128/MMBR.00031-10. Erratum in: Microbiol Mol Biol Rev. 2012 Jun;76(2):496. PMID: 21372320; PMCID: PMC3063353.
- Corti, G., Cirri, M., Maestrelli, F., Mennini, N., & Mura, P. (2008). Sustained-release matrix tablets of metformin hydrochloride in combination with triacetyl-beta-cyclodextrin. European journal of pharmaceutics and biopharmaceutics: official journal of Arbeitsgemeinschaft fur PharmazeutischeVerfahrenstechnike.V, 68(2), 303–309. https://doi.org/10.1016/j.ejpb.2007.06.004.
- Cunha V, Cotrim HP, Rocha R, Carvalho K, Lins-Kusterer L. Metformin in the prevention of hepatocellular carcinoma in diabetic patients: A systematic review. Ann Hepatol. 2020 May-Jun;19(3):232-237. doi: 10.1016/j.aohep.2019.10.005. Epub 2019 Nov 28. PMID: 31836424.
- Donadon V, Balbi M, Mas MD, Casarin P, Zanette G. Metformin and reduced risk of hepatocellular carcinoma in diabetic patients with chronic liver disease. Liver Int. 2010 (5):750-8. doi: 10.1111/j.1478-3231.2010.02223.x. Epub 2010 Mar 12. PMID: 20331505.
- De, A., Wadhwani, A., Sauraj, Roychowdhury, P., Kang, J. H., Ko, Y. T., &Kuppusamy, G. (2023). WZB117 Decorated Metformin-Carboxymethyl Chitosan Nanoparticles for Targeting Breast Cancer Metabolism. Polymers, 15(4), 976. https://doi.org/10.3390/polym15040976.
- DePeralta DK, Wei L, Lauwers GY, Fuchs BC, Tanabe KK (2014) Metformin inhibits hepatocellular carcinoma in a cirrhosis model. J Surg Res 186:63. Doi: 10.1016/j.jss.2013.11.645
- Duarah, S., Pujari, K., Ghosh, J., & Unnikrishnan, D. (2015). Formulation and Evaluation of Metformin Engineered Polymeric Nanoparticles for Biomedical Purpose. RJPBCS, 6(3), 1005-1019. ISSN: 0975-8585.
- Eskandari E, Eaves CJ. Paradoxical roles of caspase-3 in regulating cell survival, proliferation, and tumorigenesis. J Cell Biol. 2022 Jun 6;221(6):e202201159. doi: 10.1083/jcb.202201159. Epub 2022 May 12. PMID: 35551578; PMCID: PMC9106709.
- Ezzat R, Eltabbakh M, El Kassas M. Unique situation of hepatocellular carcinoma in Egypt: A review of epidemiology and control measures. World J Gastrointest Oncol. 2021 Dec 15;13(12):1919-1938. doi: 10.4251/wjgo.v13.i12.1919. PMID: 35070033; PMCID: PMC8713321.
- Foerster F, Gairing SJ, Müller L, Galle PR. NAFLD-driven HCC: safety and efficacy of current and emerging treatment options. *J Hepato*. 2022;76:446–457. [PubMed] [Google Scholar].
- Ganesan K, Rana MBM, Sultan S. Oral Hypoglycemic Medications. [Updated 2022 May 8]. In: StatPearls [Internet]. Treasure Island (FL): StatPearls Publishing; 2023 Jan-. Available from: https://www.ncbi.nlm.nih.gov/books/NBK482386/
- Garg, C., & Saluja, V. (2013). Once-daily sustained-release matrix tablets of metformin hydrochloride based on an enteric polymer and chitosan. J Pharm Educ Res. 4 (1), 92-97.
- Izabela Zarębska, Arkadiusz Gzil, Justyna Durślewicz, Damian Jaworski, Paulina Antosik, Navid Ahmadi, Marta Smolińska-Świtała, Dariusz Grzanka, ŁukaszSzylberg. The clinical prognostic and therapeutic significance of liver cancer stem cells and their marker. Clinics and Research in Hepatology and Gastroenterology, Volume 45, Issue 3, 2021, 101664, ISSN 2210-7401,https://doi.org/10.1016/j.clinre.2021.101664).https://www.sciencedirect.com/science/article/pii/S2210740121000437).
- Javidfar, S., Pilehvar-Soltanahmadi, Y., Farajzadeh, R., Lotfi-Attari, J., Shafiei-Irannejad, V., Hashemi, M., &Zarghami, N. (2018). The inhibitory effects of nano-encapsulated metformin on growth and hTERT expression in breast cancer cells. J. Drug Deliv. Sci. Technol., 43, 19-26.
- Jordan, R.I., Allsop, M.J., ElMokhallalati, Y. *et al.* Duration of palliative care before death in

international routine practice: a systematic review and meta-analysis. *BMC Med* **18**, 368 (2020). https://doi.org/10.1186/s12916-020-01829-x.

- Kafshgari, MH., Mansouri, M., Khorram, M., Samimi, A., &Osfouri, S. (2012). Bovine serum albumin-loaded chitosan particles: an evaluation of effective parameters on fabrication, characteristics, and in vitro release in the presence of non-covalent interactions. International Journal of Polymeric Materials and Polymeric Biomaterials. 61(14):1079-1090.
- Kalpna, M., Dev, D., Shahnaz, M., Parkash, J., & Prasad, D. (2018). Preparation of controlled release metformin hydrochloride loaded chitosan microspheres and evaluation of formulation parameters. Journal of Drug Delivery and Therapeutics, 8(5-s), 378-387. https://doi.org/10.22270/jddt.v8i5-s.1995.
- Kim TS, Lee M, Park M, Kim SY, Shim MS, Lee CY, Choi DH, Cho Y. Metformin and Dichloroacetate Suppress Proliferation of Liver Cancer Cells by Inhibiting mTOR Complex 1. Int J Mol Sci. 2021 ;22(18):10027. doi: 10.3390/ijms221810027. PMID: 34576192; PMCID: PMC8467948.
- Koh M. Cheryl; Chapter Eighteen-Preparation of Cells for Microscopy using 'Cell Blocks'Methods in Enzymology, Volume 533, 2013, Pages 249-255.
- Lawson DH, Gray JM, McKillop C, Clarke J, Lee FD, Patrick RS. Diabetes mellitus and primary hepatocellular carcinoma. *Q J Med.* 1986;61:945–955. [PubMed] [Google Scholar]
- Lin S, Hoffmann K, Schemmer P. Treatment of hepatocellular carcinoma: a systematic review. Liver Cancer. 2012 Nov;1(3-4):144-58. doi: 10.1159/000343828. PMID: 24159579; PMCID: PMC3760458.
- Mohammed, MA., Syeda, JTM., Wasan, KM., &Wasan, EK. (2017). An Overview of Chitosan Nanoparticles and Its Application in Non-Parenteral Drug Delivery. Pharmaceutics. 9(4):53. doi: 10.3390 /pharmaceutics9040053. PMID: 29156634; PMCID: PMC5750659.
- Mora-Huertas, C.E., Fessi, H., &Elaissari A. (2010). Polymer-based nano-capsules for drug delivery., 385(1-2), 113-142. doi:10.1016 /j.ijpharm .2009.10.018.
- Morinaga, N., Yahiro, K., Matsuura, G., Moss, J., & Noda, M. (2008). Subtilase cytotoxin, produced by Shiga-toxigenic Escherichia coli, transiently inhibits protein synthesis of Vero cells via degradation of BiP and induces cell cycle arrest at G1 by downregulation of cyclin D1. *Cellular microbiology*, *10*(4), 921-929..
- Nakatsuka T, Tateishi R. Development and prognosis of hepatocellular carcinoma in patients with diabetes. Clin Mol Hepatol. 2023 Jan;29(1):51-64. doi: 10.3350/cmh.2022.0095. Epub 2022 Jul 29. PMID: 35903020; PMCID: PMC9845683.
- Neves, A L P., Milioli, C C., Müller, L., Riella, H G., Kuhnen, N C., &Stulzer, H K. (2014). Factorial design as tool in chitosan nanoparticles development by ionic gelation technique. Colloids and Surfaces A: Physicochemical and Engineering Aspects. 445: 34-39.
- Nkontchou G, Cosson E, Aout M, Mahmoudi A, Bourcier V, Charif I, Ganne-Carrie N, Grando-Lemaire V, Vicaut E, Trinchet JC, Beaugrand M. Impact of metformin on the prognosis of cirrhosis induced by viral hepatitis C in diabetic patients. J Clin Endocrinol Metab. 2011 ;96(8):2601-8. doi: 10.1210/jc.2010-2415. Epub 2011 Jul 13. PMID: 21752887.
- Norman EML, Weil J, Philip J. Hepatocellular carcinoma and its impact on quality of life: A review of the qualitative literature. Eur J Cancer Care (Engl). 2022 Nov;31(6):e13672. doi: 10.1111/ecc.13672. Epub 2022 Aug 16. PMID: 35974658; PMCID: PMC9786637.
- Pati S, Irfan W, Jameel A, Ahmed S, Shahid RK. Obesity and Cancer: A Current Overview of Epidemiology, Pathogenesis, Outcomes, and Management. Cancers (Basel). 2023 Jan 12;15(2):485. doi: 10.3390/cancers15020485. PMID: 36672434; PMCID: PMC9857053.
- Piras, AM., Maisetta, G., Sandreschi, S., Gazzarri, M., Bartoli, C., Grassi, L., Esin, S., Chiellini, F., &Batoni, G. (2015). Chitosan nanoparticles loaded with the antimicrobial peptide temporin B exert a long-term antibacterial activity in vitro against clinical isolates of Staphylococcus epidermidis. Front Microbial. 6:372. Doi:10.3389/fmicb.2015.00372.
- Rashed, W.M., Kandeil, M.A.M., Mahmoud, M.O. *et al.* Hepatocellular Carcinoma (HCC) in Egypt: A comprehensive overview. *J Egypt*

Natl Canc Inst 32, 5 (2020). https://doi.org/10.1186/s43046-020-0016-x.

- Sabry D, Abdelaleem OO, El Amin Ali AM, Mohammed RA, Abdel-Hameed ND, Hassouna A, Khalifa WA. Anti-proliferative and anti-apoptotic potential effects of epigallocatechin-3-gallate and/or metformin on hepatocellular carcinoma cells: in vitro study. Mol Biol Rep. 2019 Apr;46(2):2039-2047. doi: 10.1007/s11033-019-04653-6. Epub 2019 Feb 1. PMID: 30710234.
- Saeedi P, Petersohn I, Salpea P, Malanda B, Karuranga S, Unwin N, et al. Global and regional diabetes prevalence estimates for 2019 and projections for 2030 and 2045: results from the international diabetes federation diabetes atlas, 9th edition. *Diabetes Res Clin Prac.* 2019;157:107843. [PubMed] [Google Scholar]
- Samuel SM, Varghese E, Kubatka P, Triggle CR, Büsselberg D. Metformin: The Answer to Cancer in a Flower? Current Knowledge and Future Prospects of Metformin as an Anti-Cancer Agent in Breast Cancer. Biomolecules. 2019 Dec 9;9(12):846. doi: 10.3390/biom9120846. PMID: 31835318; PMCID: PMC6995629.
- Sartaj A, Qamar Z, Qizilbash FF, Annu, Md S, Alhakamy NA, Baboota S, Ali J. Polymeric Nanoparticles: Exploring the Current Drug Development and Therapeutic Insight of Breast Cancer Treatment and Recommendations. Polymers (Basel). 2021 Dec 15;13(24):4400. doi: 10.3390/polym13244400. PMID: 34960948; PMCID: PMC8703470.
- Sever R, Brugge JS. Signal transduction in cancer. Cold Spring HarbPerspect Med. 2015 Apr 1;5(4):a006098. doi: 10.1101/cshperspect.a006098. PMID: 25833940; PMCID: PMC4382731.
- Sharma A, Nagalli S. Chronic Liver Disease. [Updated 2022 Jul 4]. In: StatPearls [Internet]. Treasure Island (FL): StatPearls Publishing; 2023 Jan-. Available from: https://www.ncbi.nlm.nih.gov/books/NBK554597/
- Szymczak-Pajor, I.; Drzewoski, J.; Świderska, E.; Strycharz, J.; Gabryanczyk, A.; Kasznicki, J.; Bogdańska, M.; Śliwińska, A. Metformin Induces Apoptosis in Human Pancreatic Cancer (PC) Cells Accompanied by Changes in the Levels of Histone Acetyltransferases (Particularly, p300/CBP-Associated Factor (PCAF) Protein Levels). *Pharmaceuticals* **2023**, *16*, 115. https://doi.org/10.3390/ph16010115.
- Tawfik SM, Abdollah MRA, Elmazar MM, El-Fawal HAN, Abdelnaser A. Effects of Metformin Combined With Antifolates on HepG2 Cell Metabolism and Cellular Proliferation. Front Oncol. 2022 ;12:828988. doi: 10.3389/fonc.2022.828988. PMID: 35186762; PMCID: PMC8851913.
- Tshweu, L., Katata, L., Kalombo, L., &Swai, H. (2013). Nanoencapsulation of water-soluble drug, lamivudine, using a double emulsion spray-drying technique for improving HIV treatment, J. Nanopart. Res., 15, 2040.
- Tshweu, L. L., Shemis, M. A., Abdelghany, A., Gouda, A., Pilcher, L. A., Sibuyi, N. R., Meyer M., Dube, A., & Balogun, M. O. (2020).Synthesis, physicochemical characterization, toxicity and efficacy of a PEG conjugate and a hybrid PEG conjugate nanoparticle formulation of the antibiotic moxifloxacin. RSC Adv., 10 , 19770-19780. DOI: 10.1039/D0RA08417D.
- Vacante F, Senesi P, Montesano A, Paini S, Luzi L, Terruzzi I. (2019). Metformin Counteracts HCC Progression and Metastasis Enhancing KLF6/p21 Expression and Downregulating the IGF Axis. Int J Endocrinol. 2019 Jan 10;2019:7570146. doi: 10.1155/2019/7570146. PMID: 30774659; PMCID: PMC6350585.
- Wang J, Li G, Wang Y, Tang S, Sun X, Feng X, Li Y, Bao G, Li P, Mao X, Wang M, Liu P. Suppression of tumor angiogenesis by metformin treatment via a mechanism linked to targeting of HER2/HIF-1α/VEGF secretion axis. Oncotarget. 2015 Dec 29;6(42):44579-92. doi: 10.18632/oncotarget.6373. PMID: 26625311; PMCID: PMC4792577.
- Yadav, P., Yadav, A.B. (2021).Preparation and characterization of BSA as a model protein loaded chitosan nanoparticles for the development of protein-/peptide-based drug delivery system. Future Journal of Pharmacological Sciences. 7 (200). https://doi.org/10.1186/s43094-021-00345-w.
- Younis, M K., Tareq, A Z., & Kamal, I. (2018). Optimization of swelling, drug loading and release from natural polymer hydrogels. IOP Conference Series: Materials Science and

Engineering, 454 012017. Doi:10.1088 /1757-899X/454/1/012017.

- Zhang C hao, Cheng Y, Zhang S, Fan J, Gao Q. Changing epidemiology of hepatocellular carcinoma in Asia. Liver Int. 2022 Aug 3;42(9):2029–41. Available from: https://onlinelibrary.wiley.com/doi/10.1111/liv.15251
- Zhang, Y.; Zhou, F.; Guan, J.; Zhou, L.; Chen, B. Action Mechanism of Metformin and Its Application in Hematological Malignancy Treatments: A Review. *Biomolecules* **2023**, *13*, 250. https://doi.org/10.3390/biom13020250
- Zhang Y, Wang H, Xiao H. Metformin Actions on the Liver: Protection Mechanisms Emerging in Hepatocytes and Immune Cells against NASH-Related HCC. Int J Mol Sci. 2021 May 9;22(9):5016. doi: 10.3390/ijms22095016. PMID: 34065108; PMCID: PMC8126028.
- Zou G, Bai J, Li D, Chen Y. Effect of metformin on the proliferation, apoptosis, invasion and autophagy of ovarian cancer cells. Exp Ther Med. 2019 Sep;18(3):2086-2094. doi: 10.3892/etm.2019.7803. Epub 2019 Jul 24. PMID: 31452705; PMCID: PMC6704536.